



Microgrid for Residential and Office Building with Battery Storage and Central Hot-Water Tank

Ahmad B.G. Abdalla*1, Ibrahim Aldaouab 1, Saadia K Mousa 1, Naima Hamad 1, Salah I.S. Tnatin1

¹Department of Electrical and Electronics Engineering, Omar Al-Mukhtar University, Al Baida, Libya (E-mail: ahmad.abdalla@omu.edy.ly, Ibrahim.aldaouab@omu.edy.ly, sadiya.kmees@omu.edy.ly, naima.hamad@omu.edy.ly, Salah.Tnatin@omu.edu.ly)

ABSTRACT -Renewable Energy Resources(RER) are becoming a greater fraction of the energy supply, and efficiently delivering this energy to variable loads presents a variety of problems. This paper models a small-scale microgrid consisting of residential and office building with energy supplied from solar panels, battery and hot water tank, and grid as a backup. The load profiles representing one year of building electrical and hotwater energy demand are developed from historical meter data. Electrical demand is supported by battery storage, and hotwater demand is supplied from a central storage tank. A dispatching control algorithm is designed to transfer available renewable power directly to the loads or storage systems, while confirming constraints on power flows and stored energy. For a fixed annual load profile, the proposal goal is to size system elements to minimize cost while maintaining high renewable energy penetration and low renewable curtailment. Renewable energy from a PV array is dispatched to the load or is stored for later use, and the microgrid performance is measured by the renewable energy penetration, renewable curtailment, and system cost over time. Modeling results indicate that replacing some electrical storage capacity with thermal storage for demand hotwater has the potential to decrease cost increasing renewable. penetration and decrease renewable curtailment.

Keywords: Microgrid, hot water tank, battery storage, photovoltaics, Mixed-use, renewable energy penetration, curtailment

1. INTRODUCTION

Electric power, historically is produced at a few central power stations and is transmitted long distances to end users. In recent years, this model is being replaced by decentralized or distributed electric power generation, in which power production and use are co-located [1]. Due to the decreasing costs of wind and solar energy, decentralized power often involves these technologies [1]. Because wind and solar sources are irregular, one of the main challenges to expanding distributed electricity generation is matching such variations to loads [2]. This leads to a large need for storage technology and demand response strategies [3].

The problem of integrating renewable energy into building design is relevant to this situation, because buildings consume over 40% of end-use energy worldwide [4]. There is movement in urban areas, for example, towards mixed-use buildings that combine office space and residential space [5]. Such facilities can reduce traffic congestion in dense areas by allowing workers to live closer to jobs, and they also have energyrelated benefits because residential electrical loads peak in the evening and early morning, whereas business loads generally peak in the daytime. A building design that includes both types of space will have a smoother load profile shape that is easier to integrate with a renewable energy supply.

To explore these advantages, this work models a mixeduse building whose energy needs are met with a dedicated (RER) microgrid. The building hot-water demand is met with a central hot-water tank, forming a thermal load. The microgrid supply elements consists of wind turbines, solar PV, battery storage, and grid backup. A dispatch algorithm is designed to transfer energy between these elements and building loads while managing battery level and hot water tank temperature. The microgrid performance is measured with an annual system cost, renewable penetration (the percentage of the load satisfied with RER power), and renewable curtailment (wasted RER energy). After developing a detailed system model, performance is optimized over the size of the renewable





components and dispatching parameters.

2. BACKGROUND

Distributed power systems involve engineering problems and areas of research distinct from centralized power generation. The problem of characteristics matching the electrical renewable sources to the grid are significant, such as frequency control, AC/DC conversion, etc. [6]. Peaks in the intermittent renewable power may not occur at the same time as load peaks, encouraging utilities to design ways of controlling the load with real-time pricing schemes or special deals with large business users [7]. Furthermore, there is research on controlling renewable elements themselves, such as optimal power point tracking to maximize energy transfers from wind turbines or PV arrays [8]. Renewable energy can be integrated with the full grid, or local microgrids can be designed to meet the needs of a single large building or campus [9] [10].

The problem of sizing microgrid components that include solar/wind systems with battery storage is often explored as a multi-objective optimization. For example, a grid-isolated system was optimized with the genetic algorithm (GA) to minimize annual system cost and the probability of power loss [11]. Researchers have also considered the use of forecasting to design better control algorithms for isolated microgrid operations [12] [13]. Many demand-response schemes have been studied, such as using hot-water thermal storage to create a thermal load [5].

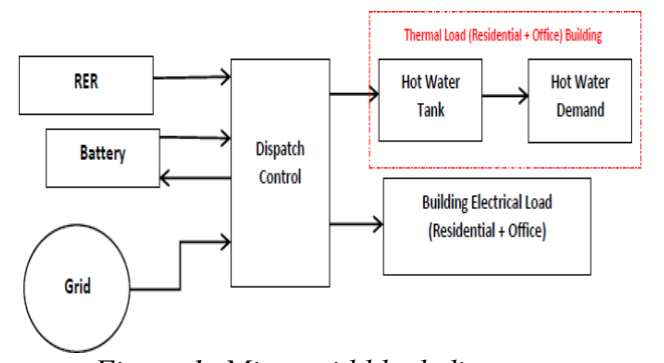


Figure 1: Microgrid block diagram.

3. MICROGRID MODEL

The specific micro-grid arrangement examined in this work is illustrated in Figure 1, with key components shown. All the arrows in this figure indicate energy transfers, on an hourly basis. Typical weather year data and models predict hourly power from the RER elements (wind and solar). A simple battery storage model is used which adjusts the current storage level each hour according to the net transfers in and out of the battery. A connection to the electrical grid provides backup power as necessary, when the RER and battery cannot meet the load. On the load side, the hot water tank and hot water load together form a thermal load. The tank needs to be maintained between 60 and 90 C^0 in order to keep a constant $60 C^0$ at the consumer's taps. The electrical load is modeled from historical residential meter data and models for office building energy demand [8] [14]. Figure 1 can be simulated with office or residential demands alone, or any mix of the two, and it can be examined with or without the hot water tank. Power from the RER that cannot be stored or used by any load is curtailed (wasted potential).

The dispatch control makes decisions about when to use battery power, when to use grid power, and when to send energy to the hot water tank (HW). These decisions can be based on the current RER output, battery charge level, tank temperature, and possibly forecasts of RER supply and building demand.

To understand the benefit of load mixing, Figure 2 shows the average daily load profile shape for the office and residential loads, along with the shape when the loads are evenly mixed. The mixed load appears slightly flatter throughout the day, on average. Computing the monthly load factors (LF) for the three loads supports this observation. LF is defined as the ratio of the average per-month consumption to the peak hourly consumption for that month. A flat, consistent electrical load will have higher LF values. Figure 3 shows the monthly LF values for the residential, office and evenly mixed loads. The mixed LF is between the office and residential values, except for 8 months March, April June, August, September and October) where the mixed LF is the largest. Including an office in the building serves to raise the LF relative to residential space alone, which is desirable because microgrid size and operating costs decrease for a higher LF.





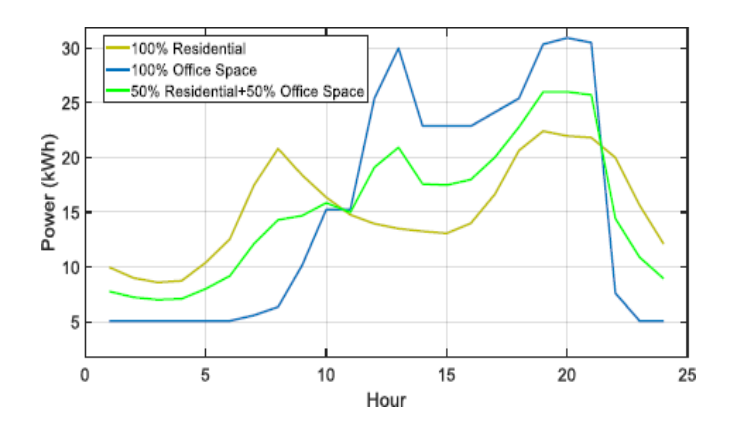


Figure 2: Average daily profiles for three loads.

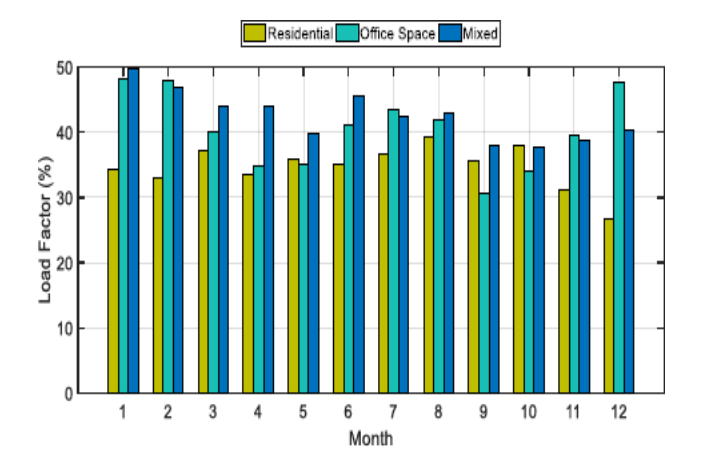


Figure 3: LF for residential, Office Spaces and combined loads.

4. COST MODEL

Parameters for the model include: number of wind turbines, PV area, battery and tank capacities, and the percentages of residential and office space loads used to make up the building load. Total annual cost is computed as the sum of an amortized capital cost and operating cost, which are both functions of the parameters N_s , N_w , B_{CAP} , and T_{CAP}. The capital cost is formed using \$1.8 per peak watt of PV power, \$22,000 per installed wind turbine (about \$2 per peak watt), \$300 for each kWh of battery capacity, and \$72 for each kWh of tank capacity [5] [8]. Standard amortization is applied with a lifetime of 20 years and an interest rate of 6% [5]. Operating costs arise from the total yearly grid power, which is purchased at a flat rate of \$0.09 per kWh.

5. DISPATCHING ALGORITHM

The dispatch control makes decisions about when to use battery power, when to use grid power, and when to send energy to the HW tank. These decisions are based on the current RER output, battery charge level, tank temperature. The dispatching algorithm splits the total RER supply components: into four (t) $P_1(t)+P_2(t)+P_3(t)+P_4(t)$. The algorithm prioritizes sending as much energy as possible directly to the load inP₁(t), and directs remaining energy to the battery P₂(t) and thermal storage P₃(t). Curtailed energy is represented by P₄(t). The level of stored battery energy each hour is represented by P_B(t), which is updated each hour according to the following equation.

$$P_{B}(t+1) = P_{B}(t) + \eta_{c}P_{2}(t) - P_{B1}(t)$$
 (1)

The quantity $P_{B1}(t)$ is the power transferred from the battery to load and η_c is charging efficiency. The battery is constrained such that $0.2B_{max} \le$ $B_{CAP}(t) \leq B_{max}$ and it cannot simultaneously be charged and discharged. In addition, the rate of energy transfer to or from the battery is constrained according to the following equation.

$$|P_B(t+1) - P_B(t)| \le 0.1B_{max}$$
 (2)

A similar model is used for the thermal storage tank, with stored energy T_{CAP}(t), charging efficiency η_{Tc} , and maximum storage capacity T_{max} (kWh).

$$P_{T}(t+1) = P_{T}(t) + \eta_{Tc}[P_{3}(t) + P_{G2}(t)] - P_{5}(t)$$
 (3)

$$0.1T_{\text{max}} \le T_{\text{CAP}}(t) < T_{\text{max}} \tag{4}$$

$$0.1T_{max} \le T_{CAP}(t) \le T_{max}$$
 (4)

$$|P_{T}(t+1) - P_{T}(t)| \le 0.1T_{max}$$
 (5)

The transfers from the tank to load are $P_5(t)$, which are taken to be the same as the load L_H(t). If renewable energy is insufficient to keep the tank minimally charged, the tank can accept backup energy transfers P_{G2}(t) from the grid. The tank needs to be maintained between 60 C⁰ and 90 C⁰ to keep a constant 60 C^0 at the consumer's taps. For a given T_{max} , this constraint leads to a tank water mass m through the equation

$$0.9T_{\text{max}} = mC_p(30C^0) \tag{6}$$

where C_p is heat capacity for water. Unlike the battery, the tank can be charged and discharged simultaneously. The electrical load must be met at each hour, such that

$$L_E(t) = P_1(t) + P_{B1}(t) + P_{G1}(t)$$
 (7)

where P_{G1}(t) is backup grid energy transfers. A





heuristic dispatch algorithm, determines all the power flows between the elements in Figure 1. At each hour t, the algorithm uses the RER output, battery charge level, tank storage level, and loads at that time to determine power dispatching. As much RER energy as possible is transmitted directly to the electrical load, with remaining energy transferred to the battery first and then the hot-water tank if any remains. The grid is used at times of low RER output and low battery charge state to satisfy the electrical load, and to ensure the tank storage level is kept above its minimum.

System performance over a period of time is described by the fraction of total RER energy that is unused (curtailment), and the fraction of the total load met with RER penetration.

$$Curtailment = \frac{\sum_{t}^{T} P_4(t)}{\sum_{t}^{T} P(t)}$$
 (8)

$$Penetration = \frac{\sum_{t}^{T} \left[P_1(t) P_{\text{B1}} \eta_{\text{Te}} + P_3(t) \right]}{\sum_{t}^{T} \left[L_{\text{E}}(t) + L_{\text{H}}(t) \right]} \quad (9)$$

It is desirable to maximize penetration while minimizing curtailment. These performance measures can be viewed as a function of the load and supply profiles (their shape and magnitude), the capacities for the two storage systems, and the dispatching algorithm. Increasing the RER output relative to the load improves penetration but raises curtailment.

6. OPTIMIZATION

Matlab© is used to simulate the power dispatching and the total system cost. System performance is measured in three ways: cost, the percentage of total RER energy that is unused (curtailment), and the percentage of the total load met with RER (penetration). These metrics can be optimized in several ways over the model parameters N_s, N_w, B_{CAP} , and T_{CAB}. In this work, cost is minimized with a lower bound on the penetration. The optimization can be performed with or without the hot-water tank included in the system, to examine the performance benefit for using a thermal load. Various optimization algorithms available in Matlab© are applied to this problem, to verify that each lead to a similar solution.

7. SIMULATION RESULTS

Figure 4 show that the dispatch algorithm ensures that the loads are met at each hour with a combination of RER energy, stored battery and thermal energy, and backup grid energy. After running the simulated microgrid for a full year, an average over the days is made. Figure 5 illustrates average daily profiles of energy transfers on the electrical side of the microgrid, clearly showing the effect of solar activity. The RER produces energy in the afternoons to support the load and charge the batteries, which then drain in the evening. Grid energy use peaks late in the day and in the morning, when storage levels are low.

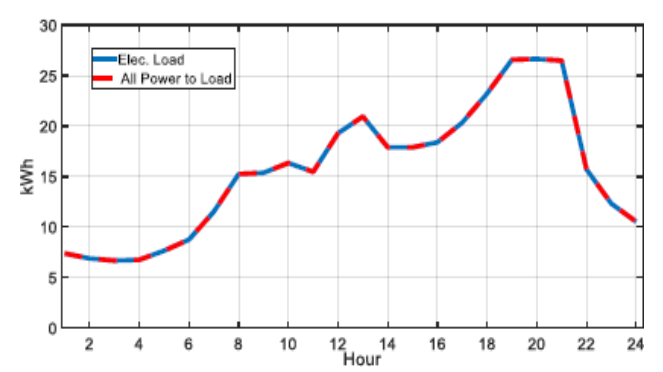


Figure 4: The average daily of electrical load and energy dispatching.

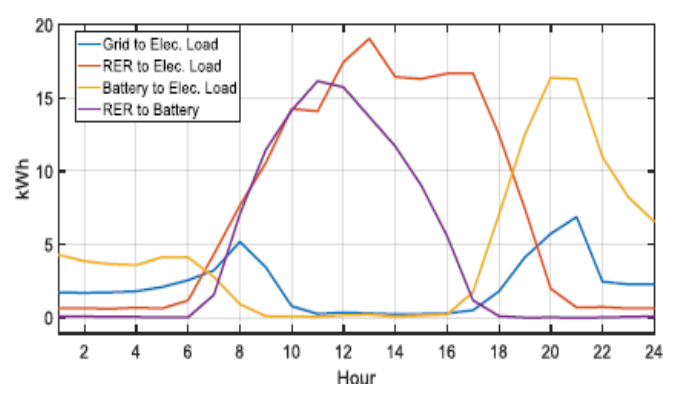


Figure 5: average daily profiles of electrical energy dispatching.

Optimization results to minimize cost at different levels of renewable penetration are shown in Figure 6. As before, results are shown for residential and office space individually, and for an even mix of the two. For each of these loads, cost is minimized at a relatively low penetration of about 20% for residential and office space loads and 40% for mixed load. This figure illustrates the cost benefit of combining the loads for higher levels of penetration. For example, at 60%





penetration, the combined load power cost is about \$0.27/kWh, and the cost for the residential power along is about \$0.34/kWh.

The advantage of mixing the loads is demonstrated by the optimization results in Table I at 60% penetration, which considers a battery only storage system (no thermal tank). The system size is optimized for three cases: residential load alone, office space load alone, and the combined (sum) load. The lowest cost per kWh occurs with the mixed load at 40% and this produces the lowest curtailment at 36%.

Table II illustrates optimization results for two cases: battery only, and battery with storage tank. For both cases, the building load is split evenly between office space and residential space, and penetration at 60%. Energy cost with battery only is \$0.21/kWh, but this decreases to \$0.19/kWh with the addition of a storage tank. The tank also serves to decrease curtailment, from 34% to 28%.

Table 1: Optimization results for separate and

тіхеа								
Load Type	Ns	N _w	B _{CAP}	Curtailment	Cost			
			(KWh)	(%)	(\$/KWh)			
Residential	188	2	160	38	0.34			
Office Space	128	1	145	36	0.27			
Mixed	234	2	228	34	0.21			

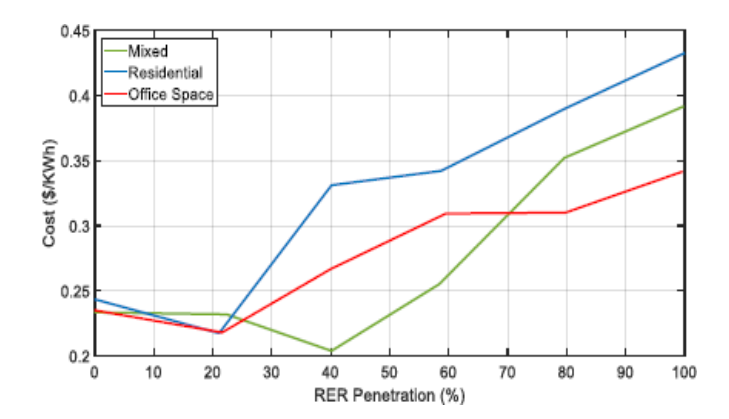


Figure 6: Average cost per kWh versus RER penetration.

Table 2: Optimization results comparing two

Storage Type	N _s	N _w	Systems B _{CAP} KWh	T _{CAB} KWh	Curtailment %	Cost \$/KWh
Battery Only	234	2	228	-	34	0.21
Battery + tank	245	1	180	48	28	0.19

8. CONCLUSION

Simulation results indicate the benefit of mixing residential with office space loads, due to the improved LF, which drives down overall energy costs. Renewable energy microgrid designs for building applications involve determining the mix of building loads to improve energy delivery.

The addition of a thermal storage tank to the microgrid allows for greater total energy storage at reduced cost, since the tank has much less cost than the battery. Unlike the battery, the tank can be charged and discharged simultaneously and it has a greater lifetime than the battery. These factors serve to reduce the total cost per kWh provided by the microgrid, while reducing curtailment.

The results presented here are based on historical —meter data to represent loads. The implementation is constructed in a modular fashion to easily incorporate changes, including: more detailed _physics for electrical and thermal storage, and dispatch algorithms that can incorporate load and —RER output forecasting. Future work will explore these modifications, along with dispatching algorithms that can utilize weather and load forecasts.

REFERENCES

- [1] B. Washom, J. Dilliot, D. Weil, J. Kleissl, N. Balac, W. Torre, and C. Richter, "Ivory tower of power: Microgrid implementation at the university of california, san diego," IEEE power and energy magazine, vol. 11, no. 4, pp. 28–32, 2013.
- [2] I. Aldaouab and M. Daniels, "Renewable energy dispatch control algorithms for a mixed-use building," in 2017 IEEE Green Energy and Smart Systems Conference IGESSC, 2017.
- [3] F. Díaz-González, A. Sumper, O. Gomis-





- Bellmunt, and R. Villafáfila- Robles, "A review of energy storage technologies for wind power applications," Renewable and sustainable energy reviews, vol. 16, no. 4, pp. 2154–2171, 2012.
- [4] S. Booth, J. Barnett, K. Burman, J. Hambrick, and R. Westby, "Net zero energy military installations: A guide to assessment and planning," National Renewable Energy Lab.(NREL), Golden, CO (United States), Tech. Rep., 2010.
- [5] I. Aldaouab and M. Daniels, "Microgrid battery and thermal storage for improved renewable penetration and curtailment," in Energy and Sustainability Conference (IESC), 2017 International. IEEE, 2017, pp. 1–5.
- [6] S. A. Raziei and Z. Jiang, "Fpga implementation of a real-time model predictive controller for hybrid power systems," in Energy Conversion Congress and Exposition (ECCE), 2017 IEEE. IEEE, 2017, pp. 3090–3097.
- [7] R. Palma-Behnke, C. Benavides, F. Lanas, B. Severino, L. Reyes, J. Llanos, and D. Sáez, "A microgrid energy management system based on the rolling horizon strategy," IEEE Transactions on Smart Grid, vol. 4, no. 2, pp. 996–1006, 2013.
- [8] I. Aldaouab, M. Daniels, and K. Hallinan, "Microgrid cost optimization for a mixed-use building," in Power and Energy Conference (TPEC), IEEE Texas. IEEE, 2017, pp. 1–5.
- [9] A. Raziei, K. P. Hallinan, and R. J. Brecha, "Cost optimization with solar and conventional energy production, energy storage, and real time pricing," in Innovative Smart Grid Technologies Conference (ISGT), 2014 IEEE PES. IEEE, 2014, pp. 1–5.
- [10] R. Almahdi and R. C. Hardie, "Recursive non-local means filter for video denoising with poisson-gaussian noise," in Aerospace and Electronics Conference (NAECON) and Ohio Innovation Summit (OIS), 2016 IEEE National. IEEE, 2016, pp. 318–322.
- [11] J. Sachs and O. Sawodny, "A two-stage model predictive control strategy for economic diesel-pv-battery island microgrid operation

- in rural areas," IEEE Transactions on Sustainable Energy, vol. 7, no. 3, pp. 903–913, 2016.
- [12] A. Raziei, K. P. Hallinan, and R. J. Brecha, "Energy cost optimization for system with both solar energy and conventional energy production and energy storage, and real time pricing," in 5th Annual Conference IEEE—Innovative Smart Grid Technologies, 2014.
- [13] R. A. Ali and R. C. Hardie, "Recursive non-local means filter for video denoising," EURASIP Journal on Image and Video Processing, vol. 2017, no. 1, p. 29, 2017.
- [14] I. Aldaouab, M. Daniels, and R. Ordóñez, "Model predictive control energy dispatch to optimize renewable penetration for a microgrid with battery and thermal storage," in Texas Power and Energy Conference (TPEC), 2018 IEEE. IEEE, 2018, pp. 1–6.